Data Combination of Infrared Thermography Images and Lock-in Thermography Images for NDE of Plasma Facing Components

Joseph MOYSAN, Cécile GUEUDRE, Gilles CORNELOUP, Laboratoire de Caractérisation Non Destructive, IUT Aix en Provence, Université de la Méditerranée, Aix en Provence, FRANCE
Alain DUROCHER, DSM/Département de Recherche sur la Fusion Contrôlée, CEA/Cadarache, Saint Paul Lez Durance cedex, France

Abstract. A pioneering activity has been developed by CEA and the European industry in the field of actively cooled high heat flux plasma facing components (PFC) from the very beginning of Tore Supra project. These components have been developed in order to enable a large power exhaust capability.
The goal of this study is to improve the Non Destructive Evaluation (NDE) of these components. The difficulty encountered is the evaluation of the junction between a carbon and a metallic substrate. This was even more difficult when complex designs have to be implemented.
A first NDE solution was based on the so called SATIR test. The method is based on infrared measurements of tile surface temperatures during a thermal transient produced by hot/cold water flowing in the heat sink cooling channel. In order to improve the definition of acceptance rules for the PFCs, a second NDE method based on Lock-in Thermography is developed. In this work we present how we can combine the two resulting images in order to accept or to reject a component. This prospective study allows improving the experimental setup and the definition of acceptance criteria.
The experimental study was conducted on trial components for the Wendelstein 7X stellarator. The conclusions will also influence future non destructive projects dedicated to the ITER project

1. Introduction

The study comes under the development of technologies for the use of controlled fusion. One of the challenges to be overcome is the confinement of particles and energy in the plasma. Specific actively cooled components must be developed: the Plasma Facing Components. These components are composed of a refractory material assembled to a heat conducting structure (copper alloy) inside of which circulates water under pressure which makes it possible to permanently evacuate the heat (cf. figure 1). Manufacturing defects may be present as a blade of air between these two materials. The inspection of the manufacturing quality of these components is crucial to guarantee the proper operation of the fusion facilities[1].

The steps for NDE assessment of the manufacturing quality proposed in this study can be applied on principle to any type of Plasma Facing Component. We present results from pre-series components of flat tile technologies in carbon fiber-carbon (CFC) intended

for a particular type of Tokamak: the Wendelstein (W7X) stellarator under construction at Greifswald in Germany [2].

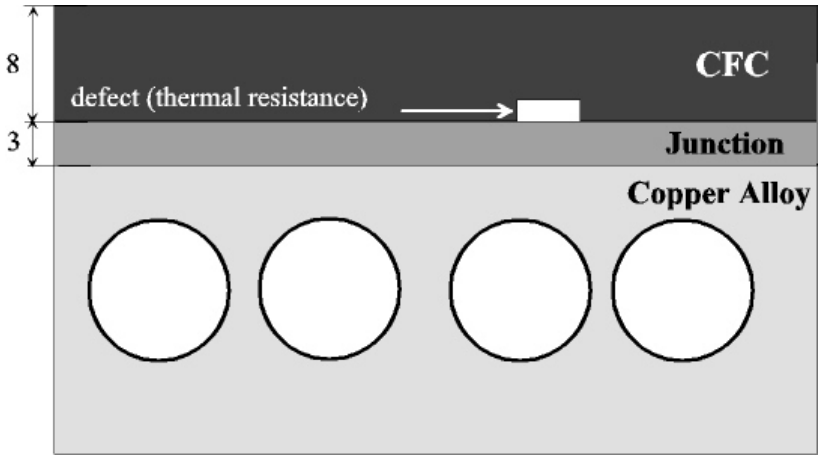

Figure 1. Simplified drawing of a section of the W7X target element and a defect.

Two infrared thermal imaging facilities were developed at CEA for the inspection of braised CFC/copper assemblies of plasma facing components. The first thermal imaging inspection device is the SATIR facility developed by the CEA for the purpose of inspecting the quality of the high flux components' assembly for the Tore Supra Tokamak [3]. The second device is an inspection method by thermal imaging modulated by external excitation; it is called the LOCKIN device.

In order to increase the performance of the methods developed at CEA, this study is interested in coupling the two methods of infrared thermal imaging previously mentioned. The coupling is done by using a data combination method to help in diagnosing the components' integrity. The data combination algorithms seeks for each anticipated decision to estimate the one which would be the most probable by combining information arising from different sources and thereby formulating a more precise diagnosis.

After this presentation of the general context of this study, in the second part we cover the experimental developments for inspecting target elements. The geometry of the component and the type of defect sought are presented first. In the third part we explain our data combination method. We close with a discussion and the perspectives for this type of process for non-destructive inspection of PFC.

2. Two infrared NDE solutions for target elements

2.1 SATIR bench

The SATIR bench is reliable and enables to do measurements of the tiles' proper assembly. The measurement principle consists of thermally exciting the cooling channels of the elements to be inspected with a cycle of hot and cold water (figure 2).

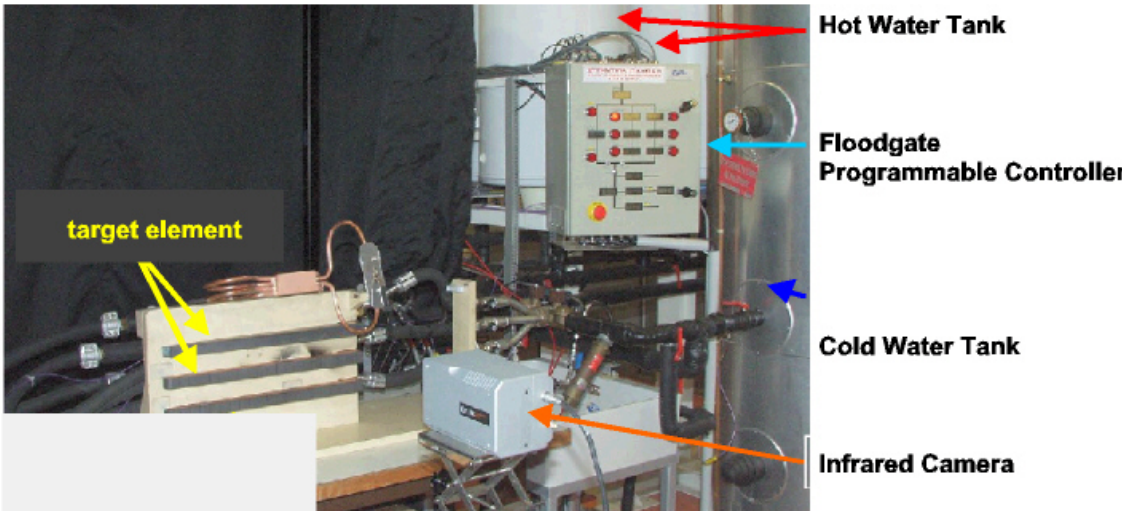

Figure 2. SATIR bench : experimental set-up

The diagnostic is prepared by comparison of the thermal transient with a reference element considered as free of defects. Any zone having an additional thermal resistance will have a slower transient temperature response than a defect free zone. The first measurement is the parameter DTref which indicates the temperature difference between the target element to be tested and the reference target element. The second measurement is Tc which is a time constant characteristic of the temperature cool down time [3]. These two measurements are calculated for each pixel of the thermal image.

2.2 LOCKIN bench

The LOCKIN bench is designed to produce a modulated thermal imaging which is based on a sinusoidal thermal excitation of the object being studied by flash lamps (Figure 3). The measurement principle consists of exciting the component by a periodic external light source while recording its temperature response by infrared thermal imaging, and then measuring the phase difference between the measured signal and the source by synchronous demodulation [4].

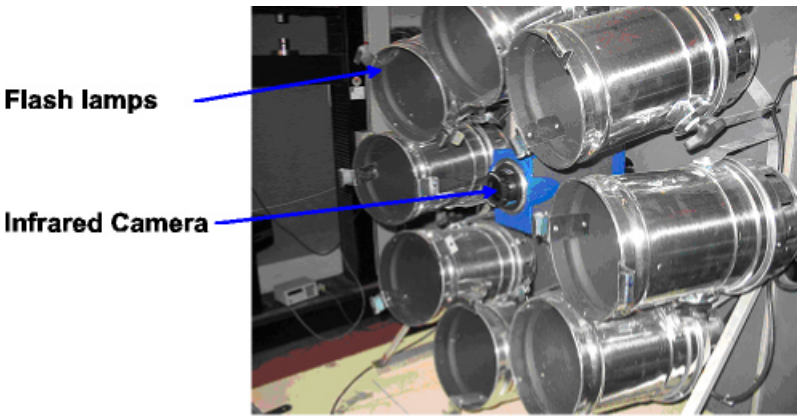

Figure 3. Set of flash lamps producing modulated thermal wave.

One of the very influential parameters is the stimulation frequency because each frequency enables to examine a different depth of the object. The frequency range used is very reduced in our application: to map all the defects with acceptable sensitivity the frequency range is located between 0.5 and 0.8 Hz. The details of perfecting this method along with the presentation of the target elements and types of potential defects are presented in reference [5].

The attenuation of the surface temperature depends on the energy absorbed and the material's properties. An interface defect locally modifies the diffusivity. The defect creates a delay in the surface's cooling or heating which is expressed in phase (degrees of angle) because the excitation is periodic. The infrared radiation issuing from each point of the object itself has a sinusoidal appearance of the same frequency, but its amplitude and delay (phase difference) can vary from one point to another. The reference is measured relative to the excitation signal. The phase difference is maximal when a defect is encountered, because the interface is considered as made of air.

The data combination method only makes sense when both methods have reliability levels of the same order of magnitude; otherwise the contribution of the method with low reliability especially risks adding noise to the method with very high reliability.

A significant work was done to define a processing procedure which makes the measurement from the new LOCKIN facility reliable. The method selected is made up of the following steps: obtaining 10 thermal imaging films, retrieval of the raw data, elimination of films showing abnormal values (the maximum phase difference observed is 30°), data filtering, for each tile eliminating the lowest and highest phase difference value (statistical sampling), and averaging the remaining values. At the outcome of this processing the averaged phase difference, denoted DPhi, is the measurement defined for each pixel of the image.

This method was tested with success on a W7X type 4B 2V target element having a natural defect. During each of the trials, the defective tile's phase difference is always greater than the normal tiles. In Figure 4, in its right part, we will analyze the infrared resulting image on three tiles, their limits are indicated with the white arrows. The central one presents a defect.

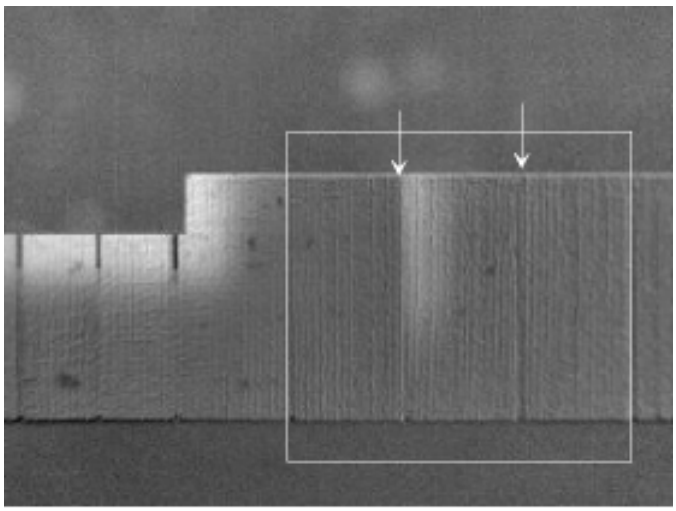

Figure 4. LOCKIN images of a W7X target element.

3. Solution for Data Combination using Dempster-Shafer rules and fuzzy logic

We have selected as data combination method the theory of belief or evidence which was developed by Shafer and Dempster on the generalization of the Bayesian theory to the management of uncertainty and ignorance [6]. It assigns degrees of confidence, called sets of mass. The combination of knowledge coming from different sensors is done through the Dempster orthogonal summation rule. The decision is made on the final set of masses as a function of the attitude adopted towards this decision (pessimistic, optimistic, etc.). This method has the advantage of being more general and adapts very well to the concept of decision thresholds used in the domain of non-destructive inspection.

Our architecture for combination is a parallel and decentralized architecture because each parallel module (SATIR and LOCKIN) provides a partial decision [7]. A pixel by pixel combination method was chosen which is more demanding in terms of relative repositioning of the two images, but less constraining a priori because there are no conditions on the objects (conductivity, size, etc.). In the architecture the redimensioning part is essential because it is necessary to assure that data that are combined come from the same spatial zone. Our method for verifying it is to use the object's characteristic points.

To adjust the data combination method the decision criteria relative to each image must be defined in advance. This part of the method requires training. Our approach is a feasibility demonstration because the number of target elements and images processed remains very low. The Dempster-Shafer method that we adopt is based on decision-making on three hypotheses. The hypothesis H_1 characterizes the presence of a defect; the hypothesis H_2 corresponds to the absence of defect; and the hypothesis H_3 corresponds to ignorance, characterizing hesitation relative to the nature of the defect.

For each measurement x_i (x_i = DTref or Tc or DPhi) limits have to be established based on which the pixel will be classified as defective, not defective or unknown (ignorance). This way three regions are defined which represents the zones where the majority decision is one of the three hypotheses H_1, H_3 or H_2 with a certainty which will be weighted by the sets of masses $M_{R_j}^{x_i}(H_i)$. The transitions between these regions are notated T_{23} (transition between region 2 and region 3) and T_{31} (transition between region 3 and region 1). If these transitions are used alone, the decision changes are very abrupt and will be too sensitive to measurement noise. To obtain a more continuous behavior from the transitions, fuzzy functions $f_{Rj}^{x_i}(x_i)$ are used. Lower (inf) and upper (sup) limits then need to be defined for each region. Figure 5 reviews a general description of these limits.

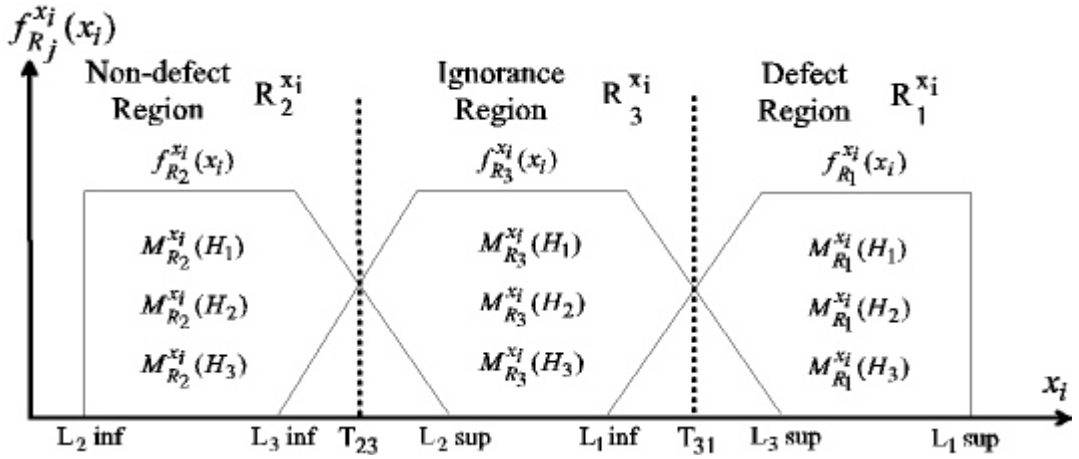

Figure 5. General description of the limits of the regions for a measurement x_i.

They are therefore a total of 24 limit values to be defined and 27 mass values. These 51 parameters are adjusted by experience, which could be done by an audit of the decision methods already in place for each technique taken separately. The method based on these three hypotheses therefore enables to use several sources of information in order to nuance a very dichotomous defect/no-defect type decision-making.

For the SATIR bench the sets of mass $M_{R_j}^{x_i}(H_i)$ are defined with the help of expertise developed in earlier studies. This tested method enables to make a very clean decision and also the size of the region $R_{H_3}^{DTref}$ is reduced to a minimum: $L_2sup = L_1inf$.

For the LOCKIN bench the sets of masses are chosen based only on the trials developed for this study. The width of the ranges $[L_{i+1}inf, L_isup]$ of fuzzy functions was chosen based on standard deviation values taken from a tile with a defect. Since the method was less tested, the values of the masses linked to ignorance are bigger than for the SATIR method.

Table 1 gives values used for the limits of the regions and indicates the sets of mass for each region and each measurement.

Table 1. Limits and Masses assigned for each decision region

	L_2inf	L_3inf	T_{23}	L_2sup	L_1inf	T_{31}	L_3sup	L_1sup
DTref	-	3.5	3.75	4	4	4.25	4.5	-
Tc	-	4.5	5.25	6	9.5	10.75	12	-
DPhi	-	6.3	7	7.7	8.7	10	11.3	-

	$M_{R_1}^{x_i}(H_1), M_{R_1}^{x_i}(H_2), M_{R_1}^{x_i}(H_3)$	$M_{R_2}^{x_i}(H_1), M_{R_2}^{x_i}(H_2), M_{R_2}^{x_i}(H_3)$	$M_{R_3}^{x_i}(H_1), M_{R_3}^{x_i}(H_2), M_{R_3}^{x_i}(H_3)$
DTref	0.9 - 0- 0.1	0- 0.9- 0.1	0- 0- 1
Tc	0.9 - 0- 0.1	0- 0.9- 0.1	0- 0- 1
DPhi	0.8- 0- 0.2	0- 0.8- 0.1	0- 0- 1

The Dempster orthogonal summation rule which enables to combine n sources of data is given in Formula (2). The purpose is to calculate the sets of mass after combination of the sources x_i for each hypothesis H_i. It is also necessary to introduce the term K which represents the conflict between the sources when they are contradictory.

$$m(H) = (m_{x_1} \oplus m_{x_2} \oplus \cdots \oplus m_{x_n})(H) = \frac{\sum_{H_i \cap H_j \ldots \cap H_n = H} m_{x_1}(H_i) \times m_{x_2}(H_j) \times \cdots \times m_{x_n}(H_n)}{1 - K} \quad (1)$$

$$\text{where} \quad K = \sum_{H_i \cap H_j \ldots \cap H_n = \varnothing} m_{x_1}(H_i) \times m_{x_2}(H_j) \times \cdots \times m_{x_n}(H_n) \quad (2)$$

In our trials, the tiles without defects do not show any noise or measurement artifacts and therefore no false defects. The mappings H_1 for the measurements DTref, Tc and DPhi are zero for these tiles. The data fusion is unnecessary in this case. The good tiles are perfectly recognized whatever the set of parameters used.

We shows in Figure 6 the results of the diagnoses (DTref, Tc, DPhi) on the central tile from Figure 4. Each result is represented in the form of maps of the hypothesis H_1 (defect present). This map therefore represents information on the confidence with which the presence of the defect is evaluated with a measurement.

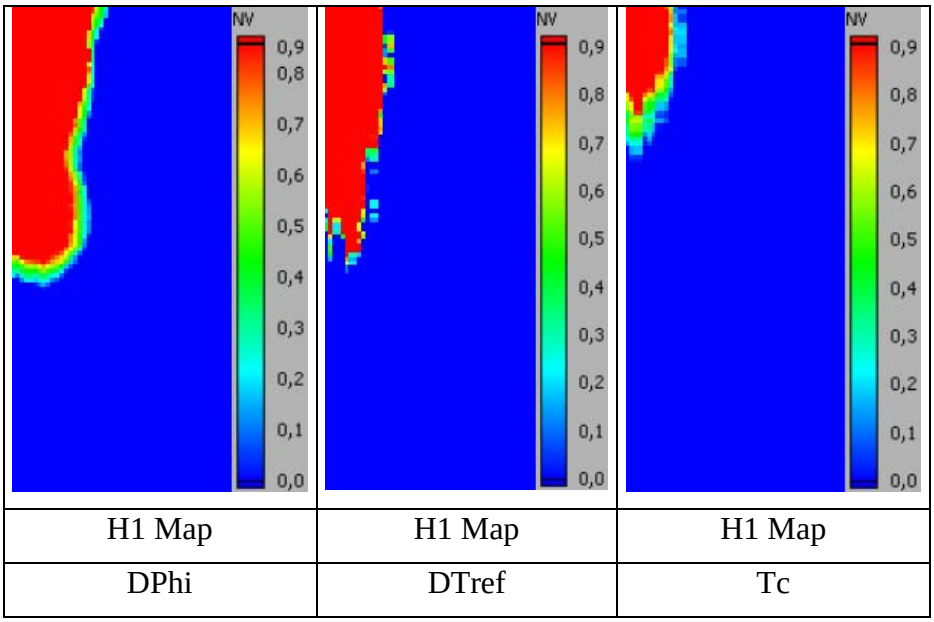

Figure 6. Mapping of the H_1 hypothesis for each measurement taken separately.

We can choose to combine the measurements coming from each infrared thermal imaging bench based on a measurement from each bench. In this study we demonstrate that if the masses express a strong confidence in the measurements and therefore that the portion of hypothesis H_3 is weak, the conflict term goes up.

To illustrate the results obtained in this study, Figure 7 shows the results of the combination based on the three measurements. Results obtained during combinations of three parameters are very encouraging and better than those from combinations with two parameters.

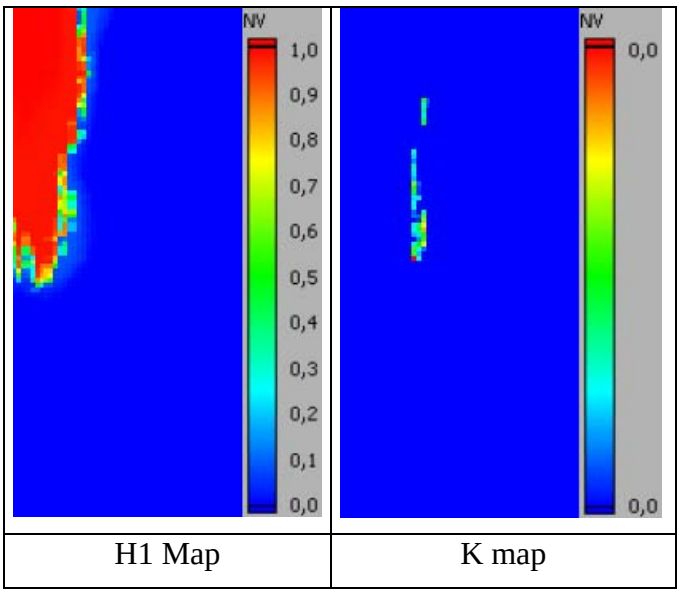

Figure 7. Mapping of hypothesis H1 and conflict K after combination of DPhi, DTref and Tc

An improvement of about 24% in the confidence is noted in the presence of a defect compared to measurements coming from the LOCKIN (DPhi) bench and 10% compared to the better measurement from the SATIR bench (DTref). We obtain a zone indicating a defect with an index of 99%.

4. Conclusions

This study shows that by using the knowledge acquired during the development of each non-destructive inspection method taken separately, it is possible to implement a process of data combination with fairly reduced training.

This process brings an improvement even for a method that is already very reliable like the method using the measurement DTref on the SATIR bench.

The study made it possible to observe that the mapping of the conflict K could be used in certain cases to delimit the defect zone. Such an approach remains exceptional to the extent that the parameters are in contradiction in the zones bordering the defect. The hypothesis H_3 is perhaps under-evaluated in this study.

Globally it would therefore be more judicious to introduce more flexibility in the masses or expand the ranges of the transition between two regions in order to propose a mapping of the combined data with less conflict. With this solution the final map of H_1 would have more reliable values.

We also conclude that we could lower the detection levels for the defects because the defect free tiles do not have measurement artifacts. The fusion methods can make it possible to use lower thresholds without systematically creating false alarms depending on the choice made for the final decision.

In light of these encouraging results, it is expected to extend this data fusion approach inspired by Dempster-Shafer to the ITER monoblock technology by combining ultrasound data with SATIR infrared thermal imaging data in order to improve the decision-making for the acceptance inspection of high-value added components.

References

[1] I. Bobin Vastra, F. Escourbiac, M. Merola, P. Lorenzetto, Activity of the European high flux test facility : FE200, Fusion Engineering and Design, 2005,

[2] H Renner et al., Divertor concept for the W7-X stellarator and mode of operation, Plasma Phys. Control. Fusion, Vol. 44, p 1005-1019, 2002

[3] A. Durocher et al., Development of an original active thermography method adapted to ITER plasma facing components control, , Fusion Engineering and Design, 75-79, 2005, p 401-405

[4] Wu D.T., Busse G., Lock-in thermography for nondestructive evaluation of materials, Revue Générale de Thermique, Vol. 37 n°8, p 693-703, 1998

[5] Durocher A., Moysan J., Escourbiac F., Missirlian M., Vignal N., Data Merging of Infrared Images for Plasma Facing Components Inspection, to be published in Fusion Engineering and Design

[6] Shafer G., International Journal Of Approximate Reasoning, 1990, 4 : 323-362

[7] Gros X.E., NDT Data Fusion, Arnold, Londres, 1997